Supplementary information

Revealing Photochromic Function and Its Physical Mechanism in Electrochromic material PEDOT:PSS

Xiangyu Ren, Shudi Lu, Kaige Huang, Jingteng Ma, Runkang Lin, Dong Hu, Xiaobao Li, Jie Yu, Yuhan Wu,* Shizhong Yue,* and Zhijie Wang**

The supporting figures

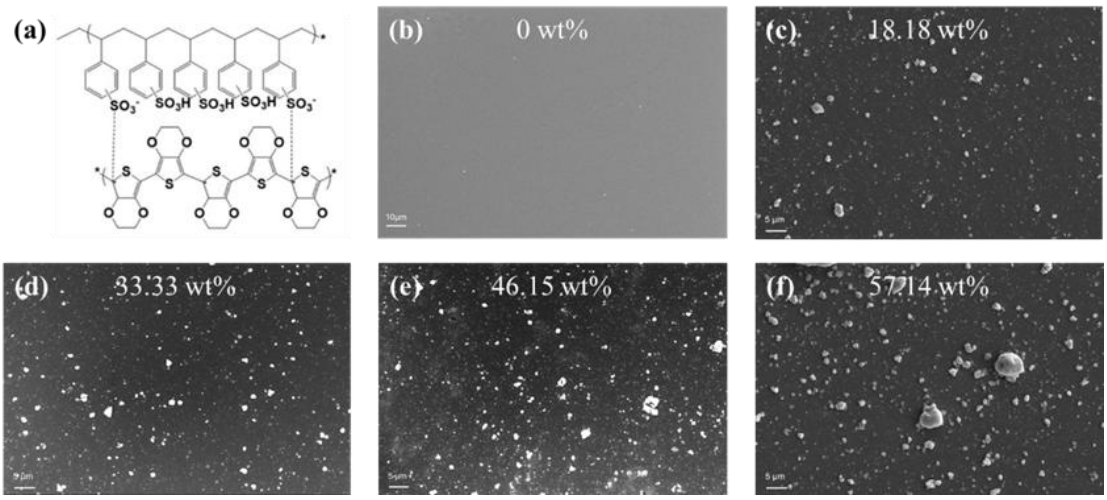

Figure S1. Chemical structure of PEDOT:PSS and SEM images of TiO_2-PEDOT:PSS films. (a) Chemical structure of PEDOT:PSS. SEM images of the PEDOT:PSS-TiO_2 film with a TiO_2 loading of (b) 0wt.%, (c) 18.18wt%, (d) 33.33wt.%, (e) 46.15wt.% and (f) 57.14wt.%.

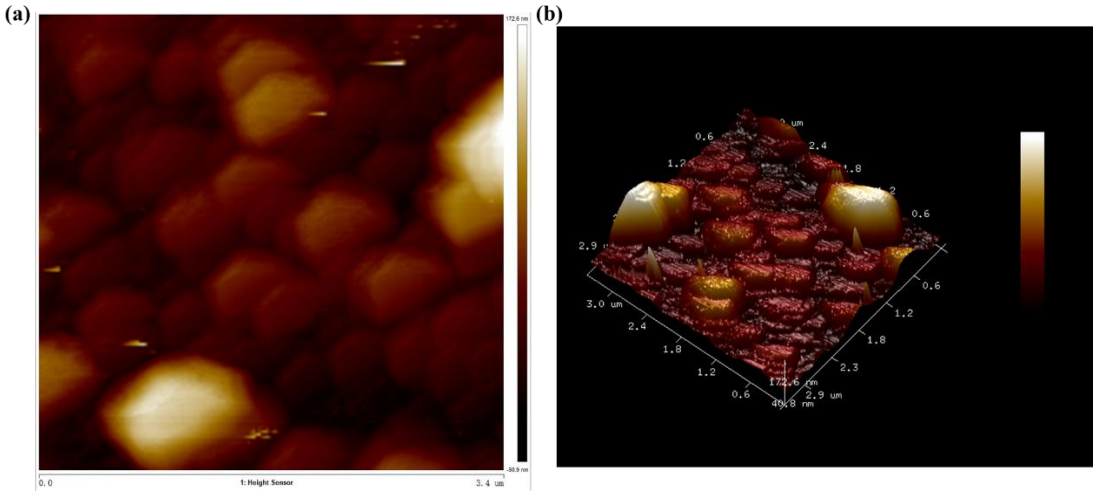

Figure S2. (a) 2D and (b) 3D AFM images of the PEDOT:PSS-TiO_2 films.

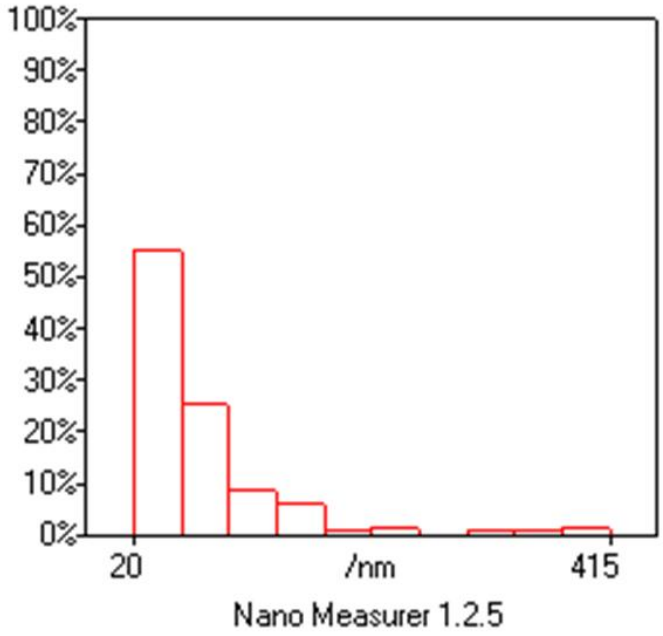

Figure S3. Surface particle size distribution of PEDOT:PSS-TiO_2 films.

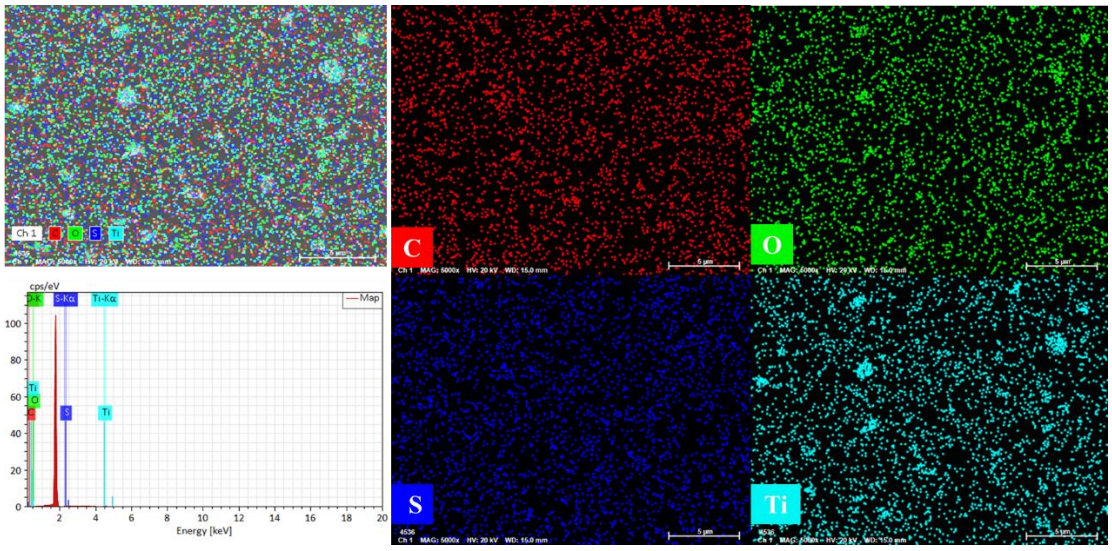

Figure S4. The EDS mapping of PEDOT:PSS-TiO_2 films for surface elemental analysis.

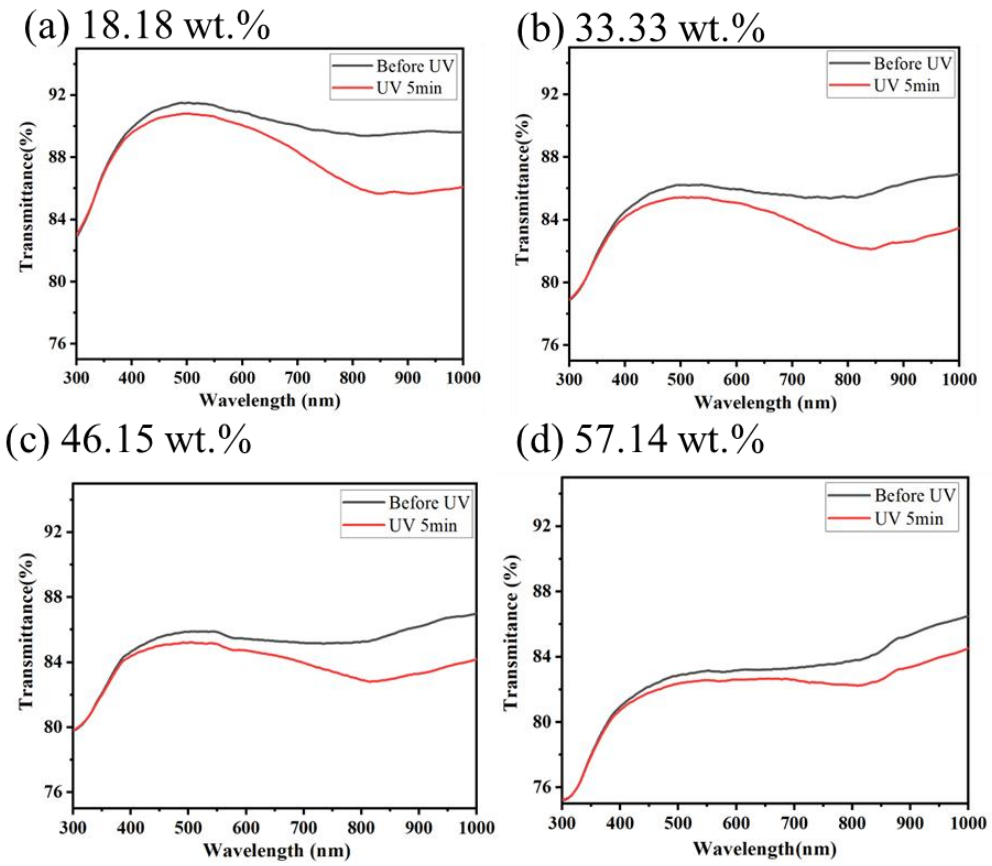

Figure S5. The transmittance of PEDOT:PSS-TiO_2 films with different TiO_2 contents before and after UV irradiation.

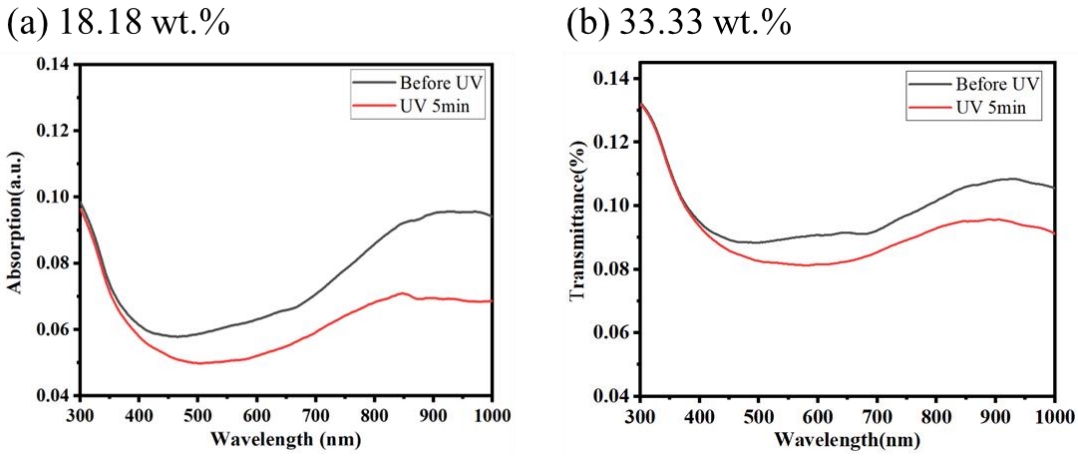

Figure S6. The UV-visible-NIR absorption spectra of PEDOT:PSS-TiO_2 films with different TiO_2 contents before and after UV irradiation.

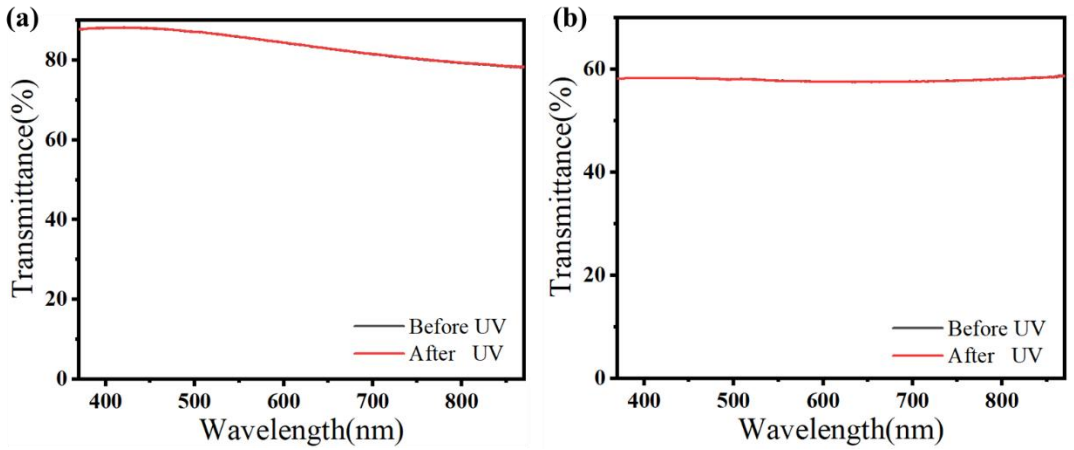

Figure S7. The transmittance of pure (a) PEDOT:PSS and (b) TiO_2 films before and after UV irradiation.

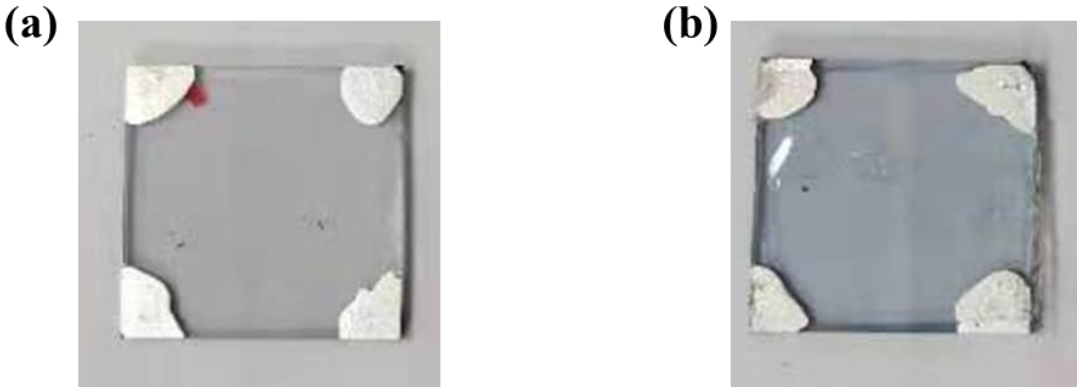

Figure S8. Color change of PEDOT:PSS-TiO_2 films (a) before and (b) after water vapor treatment under UV light irradiation.

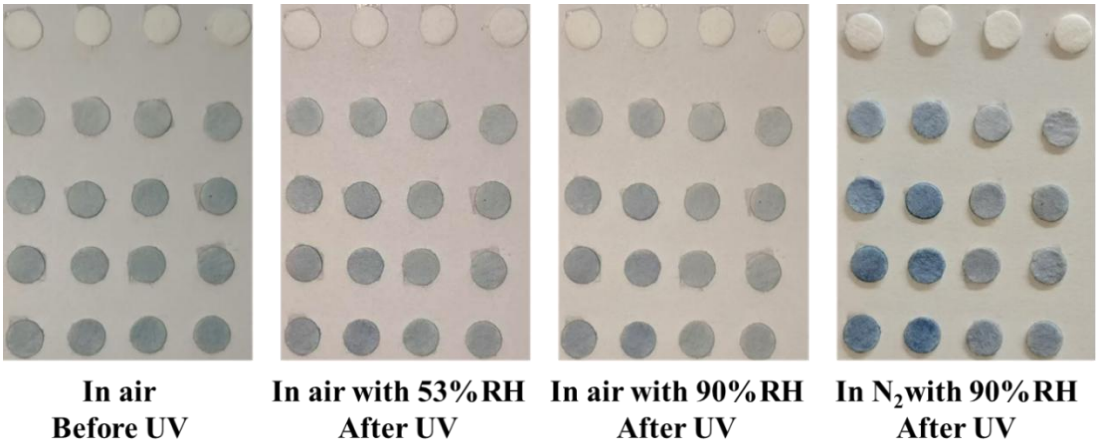

Figure S9. Optical photos of PEDOT:PSS-TiO_2 paper after UV irradiation under

different conditions.

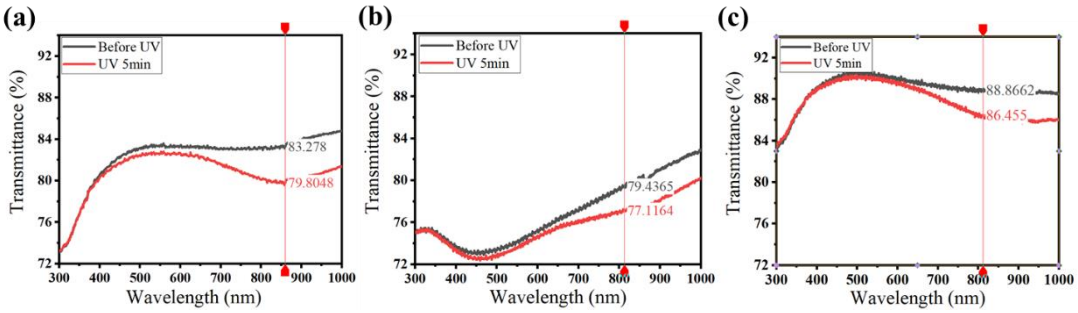

Figure S10. The transmittance of PEDOT:PSS-TiO_2 films with different crystalline types of TiO_2 before and after UV irradiation. (a) Anatase crystal type, (b) rutile crystal type, and (c) mixed crystal type.

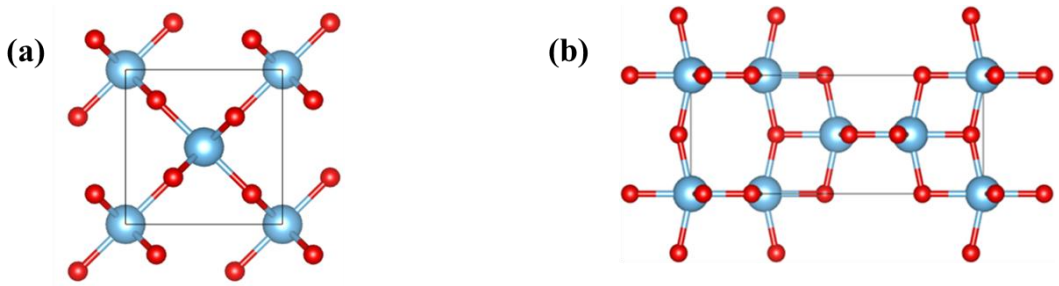

Figure S11. Crystal structure of (a) rutile and (b)anatase.

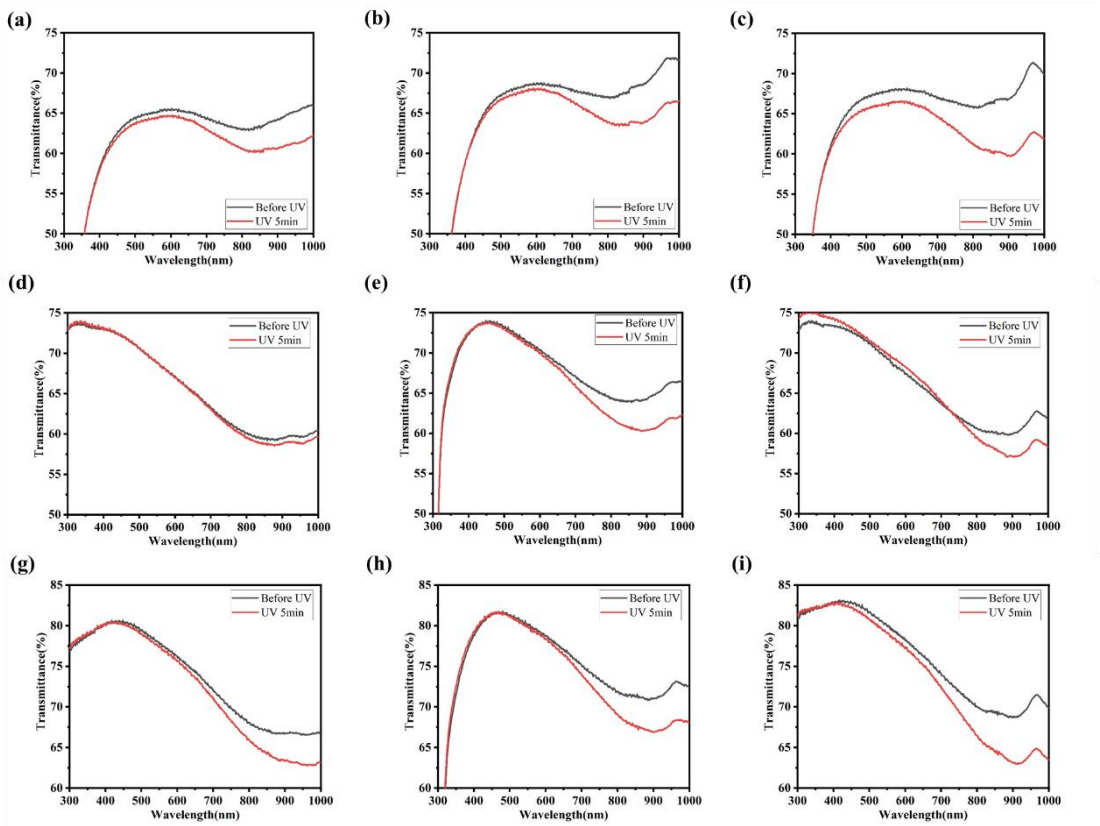

Figure S12. Effects of sacrificial agents on different TiO_2 crystal phases. The transmittance changes of anatase (a, b, c), rutile (d, e, f), and mixed-phase TiO_2 (g, h, i) occur without sacrificial agents, and when adding lactic acid and methanol as hole scavengers before and after UV irradiation, respectively.

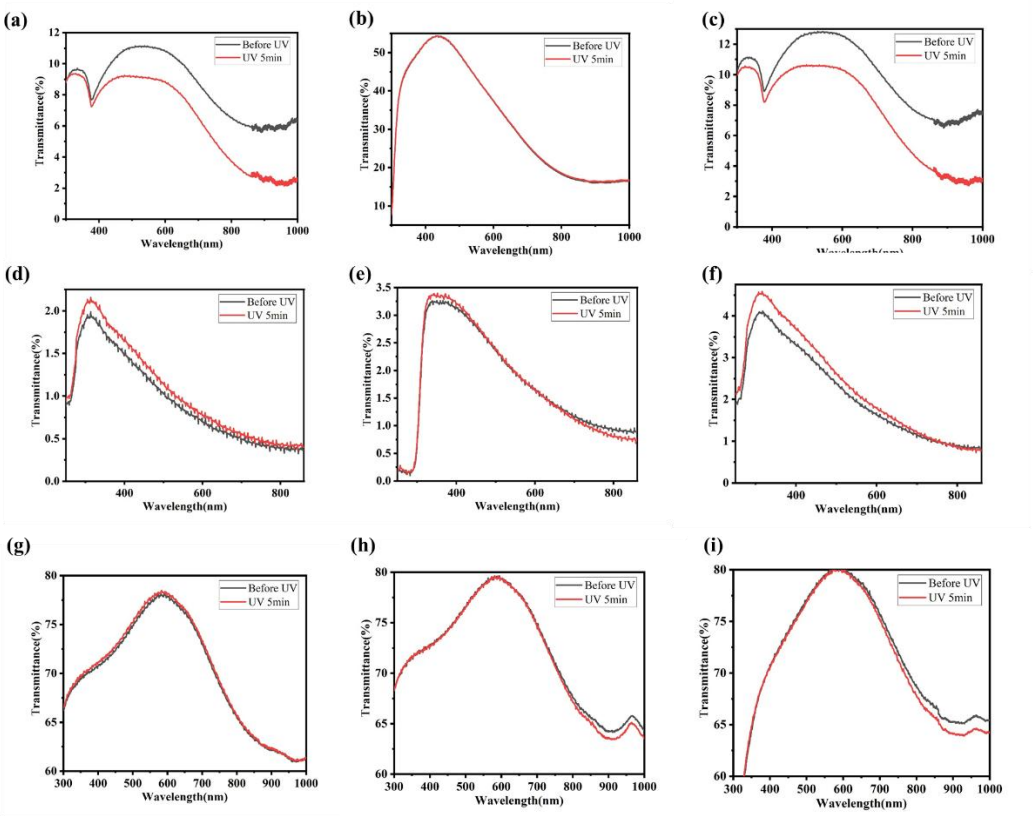

Figure S13. Effects of sacrificial agents on ZnO, CuS, and Ta_2O_5. The transmittance changes of ZnO (a, b, c), CuS (d, e, f), and Ta_2O_5 (g, h, i) occur without sacrificial agents, and when adding lactic acid and methanol as hole scavengers before and after UV irradiation, respectively.

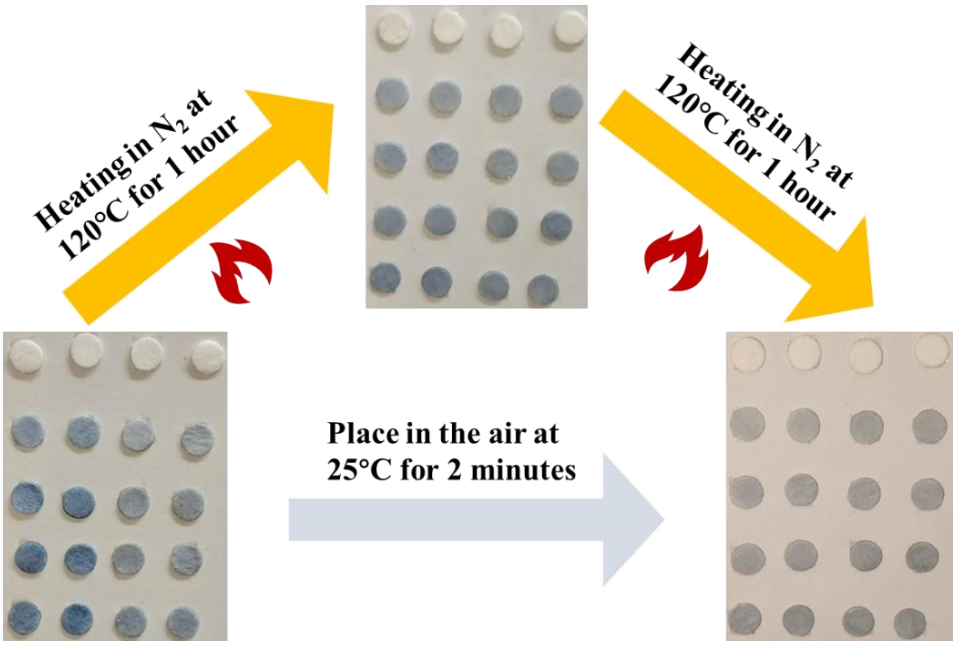

Figure S14. The reversible fading process of PEDOT:PSS-TiO_2 rewriteable paper under different conditions.

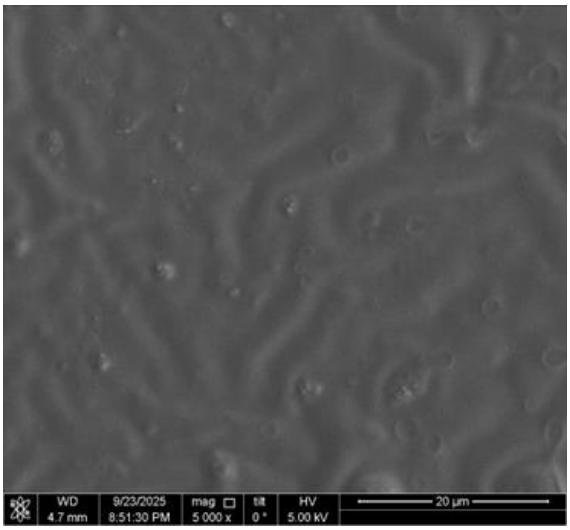

Figure S15. a) SEM images of the PEDOT:PSS-TiO2@PVP hydrogel.

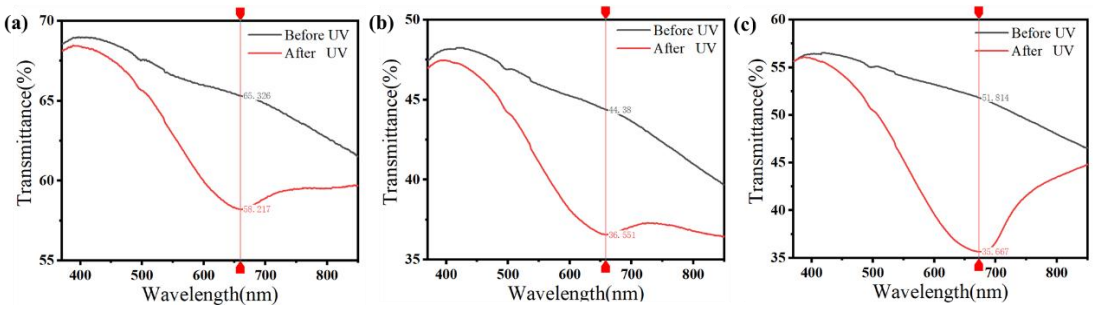

Figure S16. The transmittance of PEDOT:PSS-TiO_2@PVP hydrogel with different hydration state before and after UV irradiation. (a) dry, (b) original, and (c) wet.

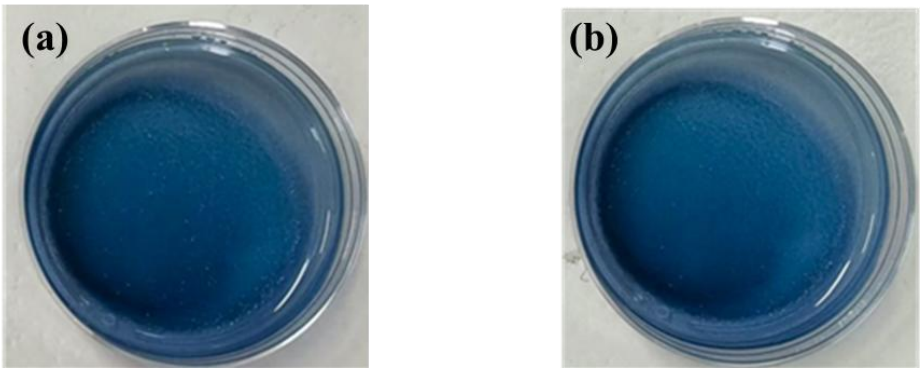

Figure S17 Optical photographs of the PEDOT:PSS-TiO_2@PVP hydrogel stored under an N_2 atmosphere. (a) initial state and (b) after one month.

State	Rutile		Anatase	
	Energy (eV)	Energy per Atom (eV/atom)	Energy (eV)	Energy per Atom (eV/atom)
Removal of 1 e^-	-58.96245	-0.19187	-116.06330	-0.00886
intrinsic (neutral)	-57.81127	0	-115.95696	0
Addition of 1 e^-	-54.37162	0.57323	-113.04212	0.24290

Table S1. Energy Change per Atom for Electron Removal and Addition